Journal of Alloys and Compounds 505 (2010) 213–216

Contents lists available at ScienceDirect

Journal of Alloys and Compounds

journal homepage: www.elsevier.com/locate/jallcom

Preparation of gadolinium gallium garnet polycrystalline powders for transparent ceramics

Guisu Wang[a], Xia Li[a,*], Yanling Geng[b]

[a] College of Materials Science and Engineering, Qingdao University of Science and Technology, Qingdao 266042, China
[b] College of Chemistry and Molecular Engineering, Qingdao University of Science and Technology, Qingdao, 266042, China

ARTICLE INFO

Article history:
Received 29 December 2009
Received in revised form 7 June 2010
Accepted 10 June 2010
Available online 16 June 2010

Keywords:
$Gd_3Ga_5O_{12}$
Co-precipitation method
Polycrystalline powder
Transparent ceramic

ABSTRACT

Gadolinium gallium garnet ($Gd_3Ga_5O_{12}$, GGG) polycrystalline powders have been prepared by a simple co-precipitation method with ammonia hydrogen carbonate as precipitant agent. XRD, FTIR, FE-SEM, TEM, and thermal analysis (TG-DTA) have been used to characterize the phase transition and morphology of the synthesized powders. Well-crystallized pure phase GGG powders were obtained at 800 °C for 2 h, without any intermediate phases formed during the process. The resultant nano-sized GGG polycrystalline powders showed good dispersion and excellent sintering activity with the particle sizes less than 100 nm.

1. Introduction

Crystalline gadolinium gallium garnet (GGG) exists in the cubic form and has a garnet structure. GGG single crystal has attracted much attention recently for its high optical and mechanical properties, such as ideal substrates for YIG magneto-optical epitaxial films and magnetic bubble memories. When doped with rare-earth ions, GGG single crystals are also widely used as laser matrix materials.

GGG single crystals are usually grown by the traditional Czochralski method. However, volatilization of the components can cause loss of stoichiometric ratio during the high temperature process, which will seriously affect the optical properties of single crystals. For refractory materials with optically isotropic lattices, ceramic techniques can offer an attractive alternative to single crystal growth. Compared to single crystal growing process, ceramic technique has several advantages, namely: (1) Ease of fabrication, no special equipment is required; (2) Availability of large-size samples with high doping concentration; (3) Realization of multi-layer active elements and multi-functional ceramics. In recent years, a new generation of solid-state laser and optical materials have received much attention due to the developing of highly transparent yttrium aluminium garnet (YAG) ceramics doped with lanthanide ions [1–7]. In 2002, Lu et al. successfully prepared highly transparent YAG ceramics using the nanocrystalline powders produced by the co-precipitation method [8]. One of the key technologies for transparent ceramics preparation is the synthesis of nano-sized powders with good dispersion and excellent sintering activity. As a result, many efforts have been made to synthesize polycrystalline GGG powders, which can be used as starting materials not only for single crystal growth but also for sintering of polycrystalline transparent ceramics. Typically, GGG powders are prepared by a solid-state reaction between the component oxides [9–11]. However, repeated milling and high temperature reaction are required.

A simple and economical method for making high quality GGG compounds is desirable, so some novel methods are developed, such as co-precipitation process [12–15], sol–gel method [16–21], solution combustion synthesis [22–27] and others [28–31]. Sol–gel method can reduce the sintering temperature, but expensive metal alkoxides are often needed as raw materials. In addition, the gel-like precursors tend to generate severe agglomeration during drying process, which will cause poor sinter activity of the resultant powders. Compared with the methods mentioned above, co-precipitation process has the advantages of low synthesis temperature and short sintering time. On the other hand, there is no need to use grinding or milling process. Such mechanical treatments may lead to surface defects and impurities, so the co-precipitation process has been developed to produce true polycrystalline materials with high homogeneity and purity.

In this paper, GGG nanocrystalline powders have been prepared by co-precipitation method at 800 °C for 2 h, with ammonium hydrogen carbonate as precipitant. The effects of synthesis conditions on the property of polycrystalline powders also have been discussed.

* Corresponding author. Tel.: +86 0532 84022772; fax: +86 0532 84022814.
E-mail address: lix@qust.edu.cn (X. Li).

0925-8388/$ – see front matter © 2010 Elsevier B.V. All rights reserved.
doi:10.1016/j.jallcom.2010.06.031

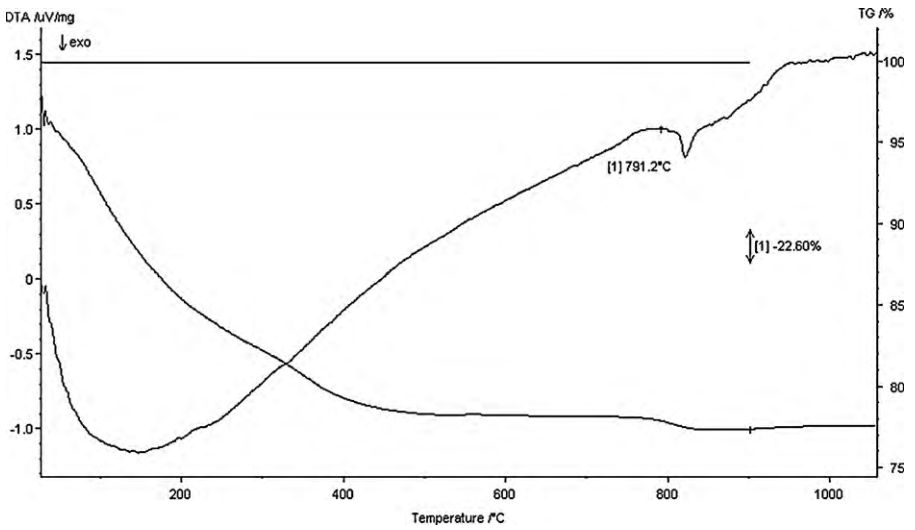

Fig. 1. TG/DTA curves of the precursor.

2. Experimental

2.1. Preparation process

Gadolinium oxide (Gd_2O_3, 99.99%) and gallium oxide (Ga_2O_3, 99.99%) were used as starting materials. Proper amounts of Gd_2O_3 and Ga_2O_3 were weighted on the basis of specific mole ratio $Gd_2O_3/Ga_2O_3 = 3:5$. Gd_2O_3 was dissolved in nitric acid solution with a concentration of 5 mol/L, and Ga_2O_3 was dissolved in concentrated nitric acid under stirring at the same time (adding appropriate ratio of hydrochloric acid). Then the as-obtained solutions were mixed together to get clarified solution. Ammonium hydrogen carbonate was gradually dropped into the mixed solution under vigorous stirring. The literature [12] reported that the pH range for co-precipitation should be controlled between 9 and 10 in theory. In our experiment, the final pH value of the solution was adjusted to about 8.5. After aging for 20 h at room temperature, the precipitate slurry was filtered, washed and dried. Then the obtained precursor was sintered in a muffle furnace at 700, 750 and 800 °C for 2 h, respectively.

2.2. Characterization

The weight loss and the heat exchange process of precursor was implemented thermogravimetry/differential thermal analysis (TG/DTA) (STA449C, Germany) in air atmosphere with a heating rate of 10 °C/min. The structures and chemical compositions of the precursors and sintered powders were measured by an American 510P type Fourier Transform Infrared Spectrometer (FTIR) (maximum resolution: 1 cm^{-1}, spectral range: 4000–400 cm^{-1}). The phase structure was identified by the X-ray diffraction (XRD) (D/MAX-II, Japan), working at 40 kV and 100 mA with the CuKα radiation (λ = 0.15418 nm) and a graphite monochromator. The particle size and morphologies of the powders were observed using transmission electron microscope (TEM) (JEM-2000EX, Japan) and field emission scanning electron microscope (FE-SEM) (JSM-6700F, Japan).

3. Results and discussion

3.1. TG-DTA analysis of precursor

Fig. 1 shows the TG-DTA curves of the precursor at a heating rate of 10 °C/min. The TG curve indicates an overall weight loss of approximately 22.60%. Much of the weight loss took place up to 400 °C corresponding to 80% of total weight loss. The weight loss that occurred below 200 °C was mainly attributed to the evaporation of absorbed water, removal of ammonia and decomposition of partial carbonate. While the weight loss that occurred at higher temperatures was mainly due to the loss of hydroxyl and decomposition of carbonate species, as suggested by Luo et al. [32]. The obvious exothermic peak centered at approximately 820 °C corresponds to the crystallization of GGG phase, which was further confirmed by the XRD results given in a later section. In fact, the crystallization temperature is often lower than that measured by DTA technique because the exothermic peak in the DTA curve often lags behind crystallization process. So, the nano-sized GGG powder can be prepared at a lower sintering temperature (800 °C) by the liquid phase co-precipitation method.

3.2. Infrared spectrum analysis

Fig. 2 shows the FTIR spectra of the precursor and GGG powders calcined at different temperatures. From the infrared spectrum of the precursor (Fig. 2a), it can be seen that the absorption peak at 3435 cm^{-1} was caused by the stretching vibration of OH^-, and the peak nearby 1635 cm^{-1} is owing to the bending vibration of OH^-. Other peaks at about 1517, 1383 and 840 cm^{-1} can be attributed to NH_4^+ and CO_3^{2-} ions in the bonding stretching mode, respectively. Thus it is certain that the obtained precursor by this method is compound carbonate, which has the lower decomposition temperature.

With the increased sintering temperature, these peaks disappeared gradually indicating that carbonate and hydroxide compounds were completely decomposed, as shown in Fig. 2b. At the same time, the characteristic vibration absorption bands of GGG phase existed. The sharp absorption peaks located at 671, 615 and

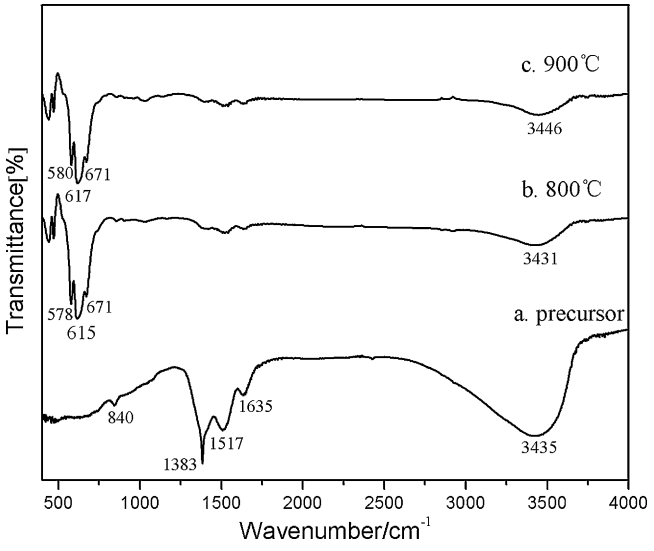

Fig. 2. FTIR spectra of the precursor and powders sintered at different temperatures.

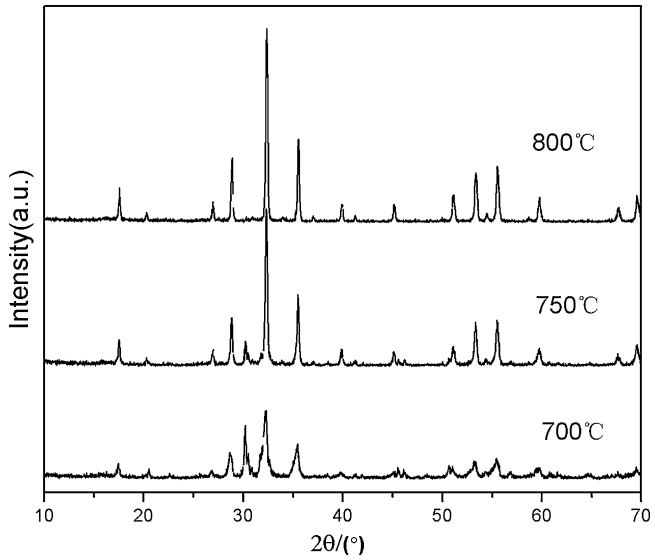

Fig. 3. XRD patterns of GGG polycrystalline samples (a) 700 °C, (b) 750 °C and (c) 800 °C.

578 cm^{-1} represent the characteristic Ga–O and/or Gd–O stretching vibrations, respectively [18]. The peaks ranged below 1000 cm^{-1} are correlated to the vibrations of the metal–oxygen bonds [33], thus they can be used to identify the phase transition process. The result is in good agreement with the XRD analysis.

3.3. XRD analysis

Fig. 3 shows the XRD patterns of the precursor powders sintered at different temperatures from 700 to 800 °C. All characteristic peaks of the diffraction patterns are consistent with that of pure GGG crystal structure (JCPDS No.13-0493), without any impurity phases. Further increasing the temperature to 800 °C, it can be seen that the intensity of GGG diffraction peaks are enhanced due to the improvement of crystallization process. The crystalline grain size of the sample is calculated by Scherrer formula using the full width at half-maximum of the (4 2 0) diffraction peak for the cubic GGG after subtraction of the equipment broadening. It is estimated that the average grain size of the sample sintered at 800 °C is about 28 nm.

The XRD results illustrated that GGG had completely formed at lower reaction temperature (800 °C) without any other intermediate phase observed. In contrast, Luo et al. [32] reported that they synthesized GGG powders from a mixed solution of Gd and Ga nitrates with stoichiometric mole ratio of 3:5 (Gd/Ga) at temperature as high as 1000 °C. Because they concluded that Ga_2O_3 exists in an approximate amorphous state and reacts with the intermediate phases to form GGG only when the temperature is higher than 800 °C:

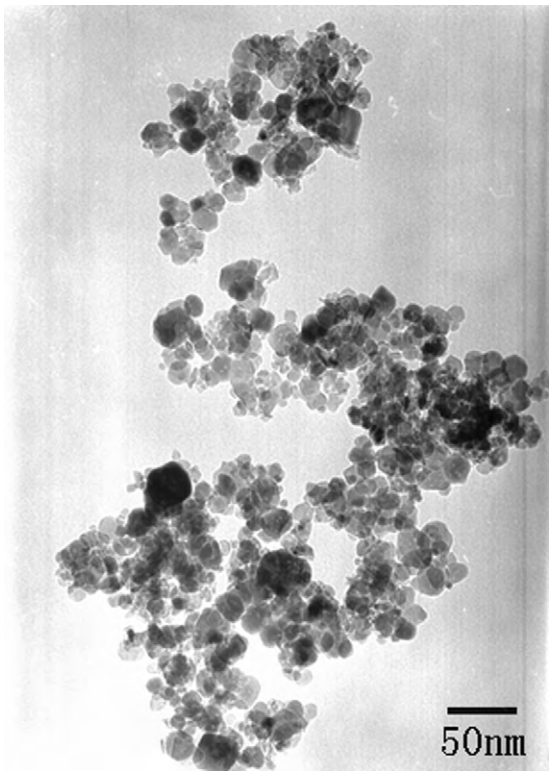

Fig. 4. TEM image of GGG polycrystalline sample sintered at 800 °C for 2 h.

$$3Gd_4Ga_2O_9 + 7Ga_2O_3 \rightarrow 4Gd_3Ga_5O_{12}$$

$$3Gd_2O_3 + 5Ga_2O_3 \rightarrow 2Gd_3Ga_5O_{12}$$

Compared with the previous reports, we have synthesized the nano-sized GGG powders at much lower sintering temperature (800 °C) for shorter holding time (2 h), without any intermediate phases formed.

The lowering of reaction temperature is attributed to the shorter diffusion distances for reactants resulting from the fine grain of the precipitated carbonate precursor. It is well known that the Ga^{3+} and Gd^{3+} ions are mixed homogeneously in liquid on the molecular level, which can shorten the ion diffusion distance. Furthermore, excessive ammonia can ensure the Ga^{3+} and Gd^{3+} is precipitated completely in the adverse titration process. Compared with $Ga(OH)_3$, the Ksp of $Gd(OH)_3$ is much lower, which can promote

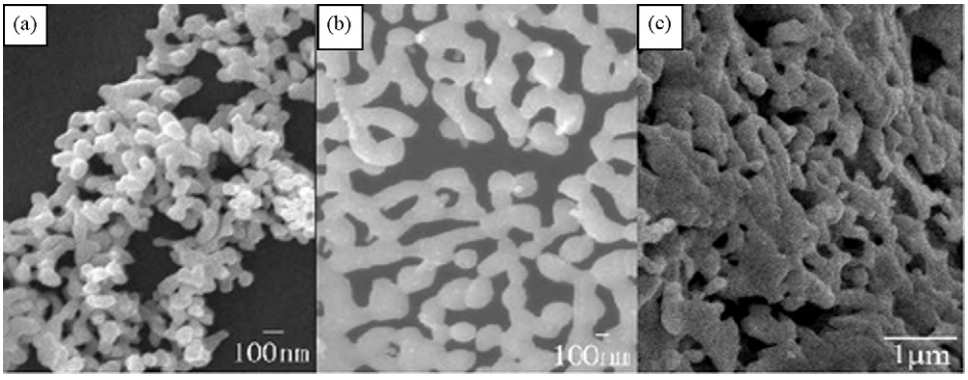

Fig. 5. SEM images of GGG polycrystalline powders (a) 800 °C, (b) 900 °C and (c) 1000 °C.

faster nucleation of $Gd(OH)_3$. So the growth of $Ga(OH)_3$ can take place on the surface on $Gd(OH)_3$ nucleus. The special core–shell structure will also shorten the diffusion distance between $Gd(OH)_3$ and $Ga(OH)_3$ molecules. Besides, as the precipitate of $Ga(OH)_3$ and $Gd(OH)_3$ was gelatinous, the special reticular structure ensures the uniformity and stoichiometric ratio of composition. All factors mentioned above contribute to reduce the reaction temperature.

3.4. Morphology characterization

The morphologies and microstructure of the as-prepared samples were investigated with TEM and SEM. Fig. 4 shows the TEM image of GGG powders sintered at 800 °C for 2 h. It can be seen directly that the as-synthesized GGG powders are loosely agglomerated with the particle sizes less than 100 nm. Fig. 5 shows the morphologies of GGG powders sintered at various temperatures. The particle sizes become gradually larger as the temperature increases, the morphologies of particles change from spherical shape to irregular one. At the same time, there are obvious neck connections to form hard aggregations. Based on the forces between co-precipitation molecules, agglomerations are mainly caused by the hydrogen bonds formed between the surface water molecules. To decrease the intermolecular surface tension, some researchers made use of ethanol and other organic solvents to remove the adsorbed water and chemical and physical coordinated water. In this paper, ethanol was also used to wash the precursor powders. Less-aggregated and better-dispersed ultra fine powders have the higher sintering activity.

4. Conclusions

The nano-sized GGG polycrystalline powders were prepared using a simple co-precipitation method. The XRD results indicated that pure GGG phase was obtained at 800 °C for 2 h. The morphology characterizations showed that the polycrystalline GGG powders had good dispersion and homogeneity with the particle sizes less than 100 nm. The resultant powders have the potential for the preparation of transparent ceramics.

Acknowledgements

This research was supported by the National Natural Science Foundation of China (NSFDYS: 50925205, Grants: 50772051, 50990303, 50872070). The authors also wish to thank the editor and anonymous reviewers for their helpful comments.

References

[1] A. Ikesue, Y.L. Aung, T. Taira, T. Kamimura, K. Yoshida, G.L. Messing, Annu. Rev. Mater. Res. 36 (2006) 397–429.
[2] A. Krell, J. Klimke, T. Hutzler, Opt. Mater. 31 (2009) 1144–1150.
[3] B.X. Jiang, W.B. Liu, T.D. Huang, J. Li, Y.B. Pan, J.K. Guo, Ceram. Int. 35 (2009) 2711–2713.
[4] M. Suáreza, A. Fernándezb, J.L. Menéndeza, R. Torrecillas, J. Alloys Compd. 493 (2010) 391–395.
[5] M. Suárez, A. Fernández, J.L. Menéndez, M. Nygren, R. Torrecillas, Z. Zhao, J. Eur. Ceram. Soc. 30 (2010) 1489–1494.
[6] Y.X. Pan, W. Wang, G.K. Liu, S. Skanthakumara, R.A. Rosenberg, X.Z. Guo, K.K. Li, J. Alloys Compd. 488 (2009) 638–642.
[7] T.D. Huang, B.X. Jiang, Y.S. Wu, J. Li, Y. Shi, W.B. Liu, Y.B. Pan, J.K. Guo, J. Alloys Compd. 478 (2009) L16–L20.
[8] J.R. Lu, K. Ueda, H. Yagi, T. Yanagitani, Y. Akiyama, A.A. Kaminskii, J. Alloys Compd. 341 (2002) 220–225.
[9] L. Kostyk, A. Luchechko, Y. Zakharko, O. Tsvetkova, B. Kuklinski, J. Lumin. 129 (2009) 312–316.
[10] E.E. Hellstrom, R.D. Rayll, C. Zhang, J. Am. Ceram. Soc. 72 (1989) 1376–1381.
[11] G.J. Zhao, T. Li, J. Xu, J. Cryst. Growth 237–239 (2002) 720–724.
[12] G.J. Zhao, T. Li, X.M. He, J. Xu, Mater. Lett. 56 (2002) 1098–1102.
[13] M. Daldosso, D. Falcomer, A. Speghini, M. Bettinelli, S. Enzo, B. Lasio, S. Polizzi, J. Alloys Compd. 451 (2008) 553–556.
[14] D.L. Sun, Q.L. Zhang, Z.B. Wang, J. Su, C.J. Gu, A.H. Wang, S.T. Yin, Mater. Sci. Eng. A 392 (2005) 278–281.
[15] M. Bazzoni, M. Bettinelli, M. Daldosso, S. Enzo, F. Serra, A. Speghini, J. Solid State Chem. 178 (2005) 2301–2305.
[16] F.P. Yu, D.R. Yuan, X.L. Duan, S.Y. Guo, X.Q. Wang, X.F. Cheng, L.M. Kong, J. Alloys Compd. 465 (2008) 567–570.
[17] W. Ryba-Romanowski, L. Lipinska, R. Lisiecki, A. Rzepka, A. Pajaczkowska, J. Nanosci. Nanotechnol. l9 (2009) 3020–3024.
[18] M.L. Pang, J. Lin, J. Cryst. Growth 284 (2005) 262–269.
[19] R. Martin-Rodriguez, R. Valiente, S. Polizzi, M. Bettinelli, A. Speghini, F. Piccinelli, J. Phys. Chem. C 113 (2009) 12195–12200.
[20] D. Hreniak, W. Strek, J. Alloys Compd. 341 (2002) 183–186.
[21] L. Yang, T.C. Lu, H. Xu, N. Wei, J. Alloys Compd. 484 (2009) 449–451.
[22] R. Krsmanovic, V.A. Morozov, O.I. Lebedev, S. Polizzi, A. Speghini, M. Bettinelli, G.V. Tendeloo, Nanotechnology 18 (2007) 1–9.
[23] F. Pandozzi, F. Vetrone, J.C. Boyer, R. Naccache, J.A. Capobianco, A. Speghini, M. Bettinelli, J. Phys. Chem. B 109 (2005) 17400–17405.
[24] R. Naccache, F. Vetrone, J.C. Boyer, J.A. Capobianco, A. Speghini, M. Bettinelli, J. Nanosci. Nanotechnol. 4 (2004) 1025–1031.
[25] R. Naccache, F. Vetrone, A. Speghini, M. Bettinelli, J.A. Capobianco, J. Phys. Chem. C 112 (2008) 7750–7756.
[26] P. Ghigna, A. Speghini, M. Bettinelli, J. Phys. Chem. C 111 (2007) 12236–12242.
[27] J.C. Boyer, F. Vetrone, J.A. Capobianco, A. Speghini, M. Bettinelli, Chem. Phys. Lett. 390 (2004) 403–407.
[28] M. Inoue, T. Nishikawa, H. Otsu, H. Kominami, T. Inui, J. Am. Ceram. Soc. 81 (1998) 1173–1183.
[29] M. Inoue, H. Otsu, H. Kominami, T. Inui, J. Mater. Sci. Lett. 14 (1995) 1303–1305.
[30] M.L. Saladino, G. Nasillo, D.C. Martino, E. Caponetti, J. Alloys Compd. 491 (2010) 737–741.
[31] L. Mancic, K. Marinkovic, B.A. Marinkovic, M. Dramicanin, O. Milosevic, J. Eur. Ceram. Soc. 30 (2010) 577–582.
[32] Z.L. Luo, M.L. Lu, J. Bao, W.H. Liu, C. Gao, Mater. Lett. 59 (2005) 1188–1191.
[33] K. Wakino, M. Murata, H. Tamura, J. Am. Ceram. Soc. 69 (1986) 34–37.